Effects of MnO$_2$ addition on microstructure and electrical properties of (Bi$_{0.5}$Na$_{0.5}$) $_{0.94}$Ba$_{0.06}$TiO$_3$ ceramics

Xiao-Juan Li · Qiang Wang · Quan-Lu Li

Abstract In this letter, MnO$_2$-doped (Bi$_{0.5}$Na$_{0.5}$)$_{0.94}$Ba$_{0.06}$-TiO$_3$ (BNBT-6) lead-free piezoelectric ceramics were synthesized by solid state reaction, and the microstructure and electrical properties of the ceramics were investigated. X-ray diffraction (XRD) reveals that all specimens take on single perovskite type structure, and the diffraction peaks shift to a large angle as the MnO$_2$ addition increases. Scanning electron microscopy shows that the grain sizes increases, and then decreases with increasing the MnO$_2$ content. The experiment results indicate that the electrical properties of ceramics are significantly influenced by the MnO$_2$ content, and the ceramics with homogeneous microstructure and excellent electrical properties are obtained with addition of 0.3 wt% MnO$_2$ and sintered at 1160°C. The piezoelectric constant (d_{33}), the electromechanical coupling factor (k_p), the dissipation factor (tan δ) and the dielectric constant (ε_r) reach 160 pC/N, 0.29, 0.026 and 879, respectively. These excellent properties indicate that the MnO$_2$-doped BNBT-6 ceramics can be used for actuators.

X.-J. Li (✉)
School of Materials and Chemical Engineering,
Xi'an Technological University,
Xi'an 710032, People's Republic of China
e-mail: xiaojuan6@yahoo.com

Q. Wang
Hefei High Magnetic Field Laboratory,
Chinese Academy of Science,
Hefei 230031, People's Republic of China

Q.-L. Li
School of Physics and Information Technology,
Shannxi Normal University,
Xi'an 710062, People's Republic of China

1 Introduction

Lead zirconium titanate (PZT) based piezoelectric ceramics are a high-performance piezoelectric materials, which are widely used in sensors, actuators, transducers and other electronic devices. However, PZT piezoelectric ceramics contain more than 60 weight percent lead, and the waste of products containing Pb cause a crucial environmental problem under ground water. Lead has recently been expelled from many commercial applications and materials (for example, from solder, glass and pottery glaze) owing to concerns regarding its toxicity. The legislation will be enforced in the EU as the draft directives on waste from electrical and electronic equipment (WEEE), restriction of hazardous substances (ROHS) and end-of life vehicles (ELV) [1, 2]. Therefore, it is necessary to develop environment-friendly lead-free piezoelectric ceramics to replace the PZT-based piezoelectric ceramics, which has became one of the main trends in present development of piezoelectric materials.

Bismuth sodium titanate, Bi$_{0.5}$Na$_{0.5}$TiO$_3$ (BNT), developed by Smolenskii with a rhombohedral perovskite structure has relatively large remnant polarization ($p_r = 38 \mu C/cm^2$) at room temperature and high Curie temperature T_C =320°C [3]. In addition, BNT ceramics reveals an anomaly in its dielectric properties as a result of low-temperature phase transition from the ferroelectric to the antiferroelectric phase at about 200°C, which can be called depolarization temperature T_d. The T_d is an important factor for BNT and BNT-based ceramics in view of their practical use because the piezoelectric signal disappears

above T_d [4]. Therefore, it has been considered to be a good candidate for lead-free piezoelectric ceramics. However, pure BNT ceramics is hard to be poled and its piezoelectric properties is not desirable because of its relatively large coercive field (E_r=7.3 kV/ mm). To improve piezoelectric and dielectric properties of BNT ceramics, various BNT-based solid solutions have been developed [5–9]. Among these solid solutions, $(Bi_{0.5}Na_{0.5})_{1-x}Ba_xTiO_3$ (BNBT-x) system has attracted a great deal of attention owing to the existence of a rhombohedral-tetragonal morphotropic phase boundary (MPB) near x=0.06~0.08. Compared with pure BNT, the BNBT-x composition piezoelectric ceramics reveal relatively high piezoelectric properties and low coercive field near the MPB. Takenaka T et al. [5] reported that BNBT-6, which is near the MPB, has relatively good piezoelectric properties: d_{33}=125 pC/N, k_{33}=0.55. Although BNBT-x ceramics possess good piezoelectric properties near the MPB, the gap is still existent comparing with PZT. To further enhance the properties of BNBT-x ceramics, some additions have been used for the specific application [10–16]. Pengpat K [12] reported the effect of La_2O_3 additive on piezoelectric properties of BNBT-x ceramics. It was found that the dissipation factor tan δ was decreased and the piezoelectric constant d_{33} was increased up to 112 pC/N. H. D. Li [13] and B. J. Chu [14] used Nb_2O_5 as modifier for BNBT-x ceramics and found that the Nb^{5+} not only enhanced piezoelectric coefficient (d_{33}= 149 pC/N, k_p=0.2), but also enhanced dielectric loss (tan δ= 4.6%). Wang et al. [15] and Wu et al. [16] also researched the effect of CeO_2 additions on microstructure and electrical properties of BNBT-x ceramics and obtained the better piezoelectric properties. In addition, KBT modified BNBT material is also an important family and effectively improve the piezoelectric properties. Nagata et al. [17] reported that the enhancement can be found in the piezoelectric properties in the $(Bi_{1/2}Na_{1/2})TiO_3$–$(Bi_{1/2}K_{1/2})$ TiO_3–$BaTiO_3$ (abbreviation BNT–BKT–BT) system. Y. M. Li et al. [18] investigated $(1-5x)$ BNT–$4x$KBT–x BT lead-free ceramics system. It was found that the best piezoelectric constant d_{33}=149 pC/N at x=0.030 and planar electromechanical coupling factor k_p=0.282 at x=0.028 were observed. S. J. Zhang et al. [19] researched recently x $(Na_{0.5}Bi_{0.5})TiO_3$-y$(K_{0.5}Bi_{0.5})TiO_3$-z$BaTiO_3$ $[x + y + z = 1; y : z = 2 : 1]$ system and found the piezoelectric constant d_{33}=170 pC/N and coercive field E_r=2.9 kV/mm at x= 0.88.

MnO$_2$, as a dopant, is widely used in PZT and PZT-based ceramics to improve the piezoelectric properties. Kamiya et al. [20] studied deeply the effects of MnO_2 doping on piezoelectric properties of PZT. They found that MnO_2 not only increased the piezoelectric properties of PZT, but also displayed properties of "soft" and "hard" doping simultaneously. However, researches of MnO_2-

doped BNT-based ceramics are scarce. In this paper, MnO$_2$-doped BNBT-6 lead-free piezoelectric ceramics were synthesized by conventional ceramic fabrication technique. The effects of MnO_2 content on the phase structure, microstructure, dielectric and piezoelectric properties of BNBT-6 ceramics were studied in detail. The optimum conditions, including MnO_2 addition content and sintering temperature, were obtained.

2 Experiment

The conventional mixed-oxide method was used to prepare BNBT-6+$x$wt%MnO$_2$ (x=0~0.45) ceramics. Reagent-grade Bi_2O_3 (98.92%), Na_2CO_3 (99.8%), TiO_2 (99%), $BaCO_3$ (99.8%), and MnO_2 (90%) were used as starting materials. These materials were weighted according to the above compositional formula and mixed in distilled water with carnelian balls by ball milling for 6 h, then dried and calcined at 850°C for 2 h in air. The calcined powders were re-milled and mixed with a PVA binder solution, then pressed into discs with 20 mm in diameter and 1~2 mm in thickness under 176 MPa uniaxial pressure. Through a 500°C binder burnout, these samples were sintered at 1140°C~ 1200°C for 40 min in air.

The bulk densities of samples were measured by the Archimedes method. The crystal structures of sintered samples were confirmed using an x-ray diffraction-meter with a nickel-filtered Cu $K\alpha$ radiation (D/max-2550/pc, Rigaku Company, Japan). In order to determine the phase structure of the ceramics, fine scanning was recorded in the ranges of 39°–41° and 45°–48°. The microstructures of samples were observed with scanning electron microscope (Quanta 200, Philips-FEI Company, Holand).

Fired-on silver paste was used as electrodes for the measurement of the dielectric properties and piezoelectric
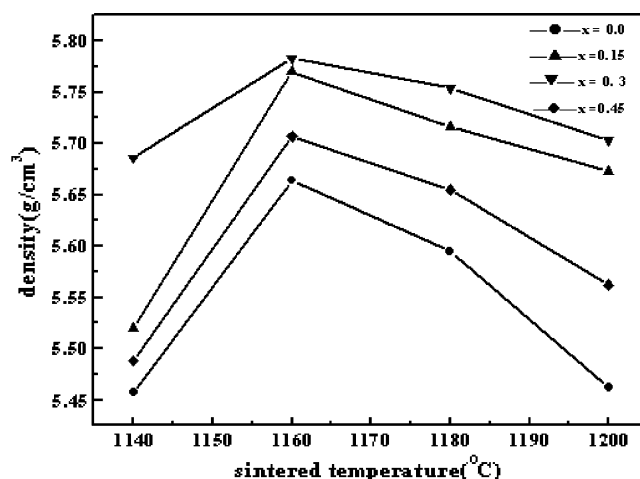

Fig. 1 Bulk density of BNBT-6 + $x$wt%MnO$_2$ (x=0, 0.15, 0.3, 0.45) ceramics as a function of sintering temperature

properties of sintered samples. Ceramic samples were poled under a dc electric field of 3~6 kV/mm at 80°C in a silicon oil bath for 20 min. After laying a day, the piezoelectric constant (d_{33}) was measured using a quasi-static piezoelectric d_{33}-meter (ZJ-4, Institute of acoustics, Chinese Academy of Sciences). The free relative permittivity (ε_r) and loss tangent (tan δ) of the samples were measured at 1 kHz using an impedance analyzer (Angline, HP 4294A). The planar electromechanical coupling factor (k_p) and mechanical quality factor (Q_m) were determined using the impedance analyzer according to the resonance–antiresonance method [21].

3 Results and discussion

Figure 1 gives the bulk density of BNBT-6 + $x$wt%MnO$_2$ (x=0, 0.15, 0.3, 0.45) ceramics as a function of sintering temperature. It can be seen that the density of all specimens increases rapidly with sintering temperature range from 1140°C to 1160°C. However, further increasing sintering temperature above 1160°C makes them all decreases, which is most probable due to mass loss of Bi_2O_3 (volatilization temperature 1130°C).

In addition, Fig. 1 also indicates the density of BNBT-6 + $x$wt%MnO$_2$ (x=0, 0.15, 0.3, 0.45) ceramics as a function of MnO$_2$ addition at the same temperature. As can be seen from the figure, the density of specimens presents a increasing trend for small addition less than 0.3 wt%, then a decreasing trend for x >0.3 wt%, and the max of density is 5.783 g/cm^3 for x=0.3 wt% at 1160°C. It means that the suitable MnO$_2$ addition benefits the densification of ceramics during the sintering process. However, excessive addition of MnO$_2$ leads to a decrease in the density of ceramics. It is supposed that the grain sizes increase and become homogeneous with small addition of MnO$_2$ less than 0.3 wt%. However, further increasing amount of MnO$_2$ above 0.3 wt% inhibits the grain sizes lessening and leads to the inhomogeneous of grain distributing [22]. From above results, it is expected that MnO$_2$ has solubility

Fig. 2 (a) XRD patterns in the 2θ ranges of 20–80° and (b) the fine scanning in the 2θ ranges of 39–41° and 45–48° of BNBT-6 + $x$wt%MnO$_2$ (x=0, 0.15, 0.3, 0.45) ceramics sintered at 1160°C


(a)

(b)
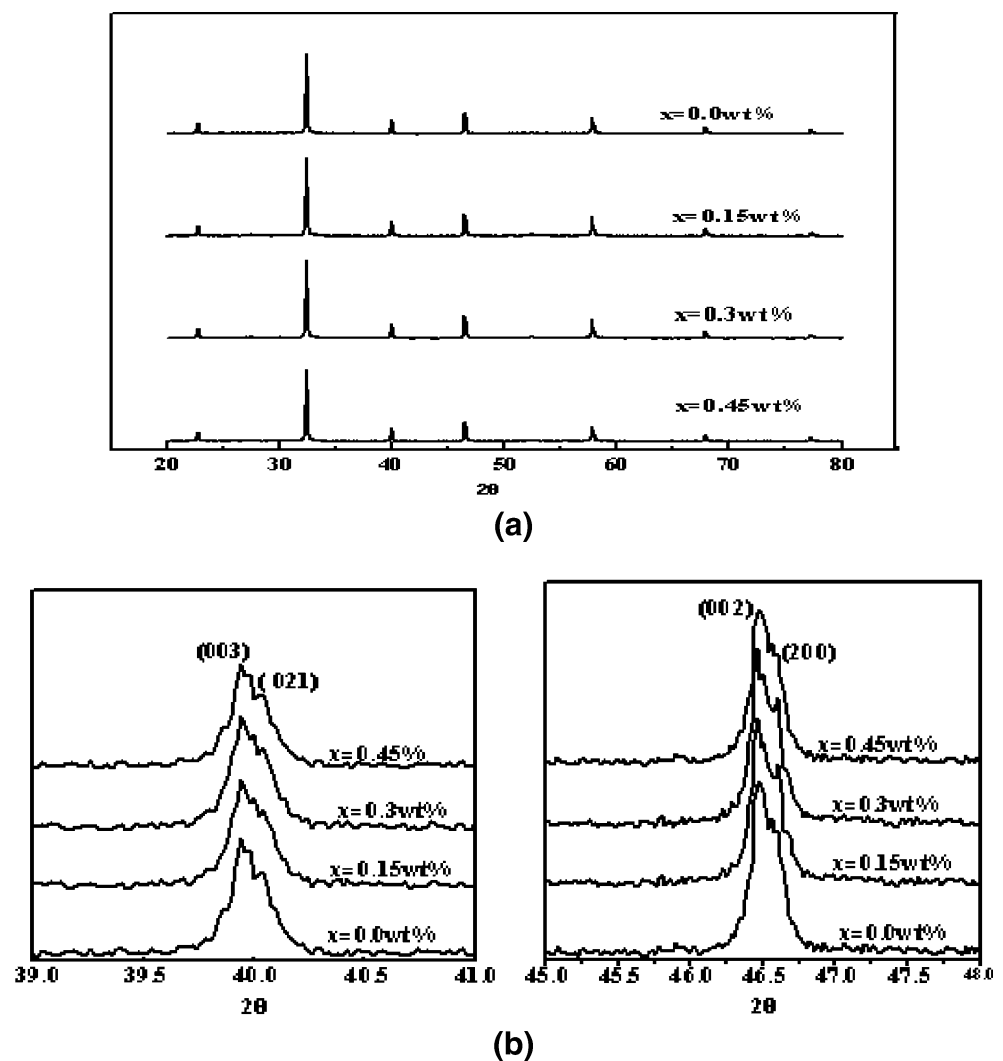
of about 0.3 wt% and sintering temperature is at 1160°C in BNBT-6 ceramics.

Figure 2(a) and (b) show the XRD and the fine scanning of BNBT-6+$x$wt%MnO$_2$ (x=0, 0.15, 0.3, 0.45) ceramics sintered at 1160°C, respectively. From Fig. 2(a), it can be seen that all samples display a pure perovskite structure without any secondary impurity phases, which indicates that Mn ion diffuses into the lattice of BNBT-6 to form solid solution, but does not affect the structure of BNBT-6 during sintering. Figure 2(b) gives the fine scanning of ceramics in the 2θ ranges of 39°–41° and 45°–48°, respectively. It can be clearly seen that the (003), (021) reflections of the rhombohedral phase and the (002), (200) reflections of the tetragonal phase appear near 40° and 46.5°, respectively. This result shows that all samples exhibit the coexistence of a rhombohedral–tetragonal phase. On the other hand, it can be seen that the diffraction peaks shift to the higher angle with increasing amount of MnO$_2$ doping, which indicates the decrease of lattice constant as the addition MnO$_2$ increased. Generally, Mn ions exist in Mn^{2+} and Mn^{3+} in the perovskite structure and enter into the lattice to substitute B-site ions because the radius of Mn^{2+}(0.08 nm) and Mn^{3+} (0.066 nm) is close to that of Ti^{4+}(0.068 nm), which brings oxygen vacancy to cause distortion of the crystal lattices of the BNBT-6 ceramics [23].

Figure 3 shows the SEM micrographs of the BNBT-6 + $x$wt%MnO$_2$ (x=0, 0.15, 0.3, 0.45) ceramics sintered at 1160°C. It can be observed from Fig. 3(a) that distinct pores exist for un-doped ceramics. Comparatively, the surfaces of specimens doped with 0.15 wt% and 0.3 wt% MnO$_2$ are more uniform as seen in Fig. 3(b) and (c), respectively. Furthermore, the grain sizes of ceramics increase by increasing amount of MnO$_2$ addition. However, the grain sizes reduce further increasing the amount of MnO$_2$ to 0.45 wt% as seen in Fig. 3(d). It is obvious that the above results are consistent with the change in the density with MnO$_2$ content for Mn-doped BNBT-6 specimens, as shown in Fig. 1. As stated above, Mn ions will enter into the perovskite lattice to substitute B-site ions for x<0.3 wt%. The unbalance of ion valence leads to the creation of oxygen vacancies, which enhances the transfer of mass and energy between reactants, thus improving the sintering behavior and inducing an increase in grain size. However, excessive doping will drastically worsen the sintering behavior of the ceramics because a great deal MnO$_2$ congregate in the grain boundary [24, 25].

Figure 4 shows the piezoelectric constant d$_{33}$ and the electromechanical coupling factor k_p of BNBT-6 ceramics sintered at 1160°C as a function of MnO$_2$ addition. It can be seen that d$_{33}$ and k_p show almost the same trend with

Fig. 3 SEM micrographs of BNBT-6 + $x$wt%MnO$_2$ (x=0, 0.15, 0.3, 0.45) ceramics sintered at 1160°C: (**a**) x=0.0 wt%; (**b**) x=0.15 wt%; (**c**) x=0.3 wt%; (**d**) x=0.45 wt%
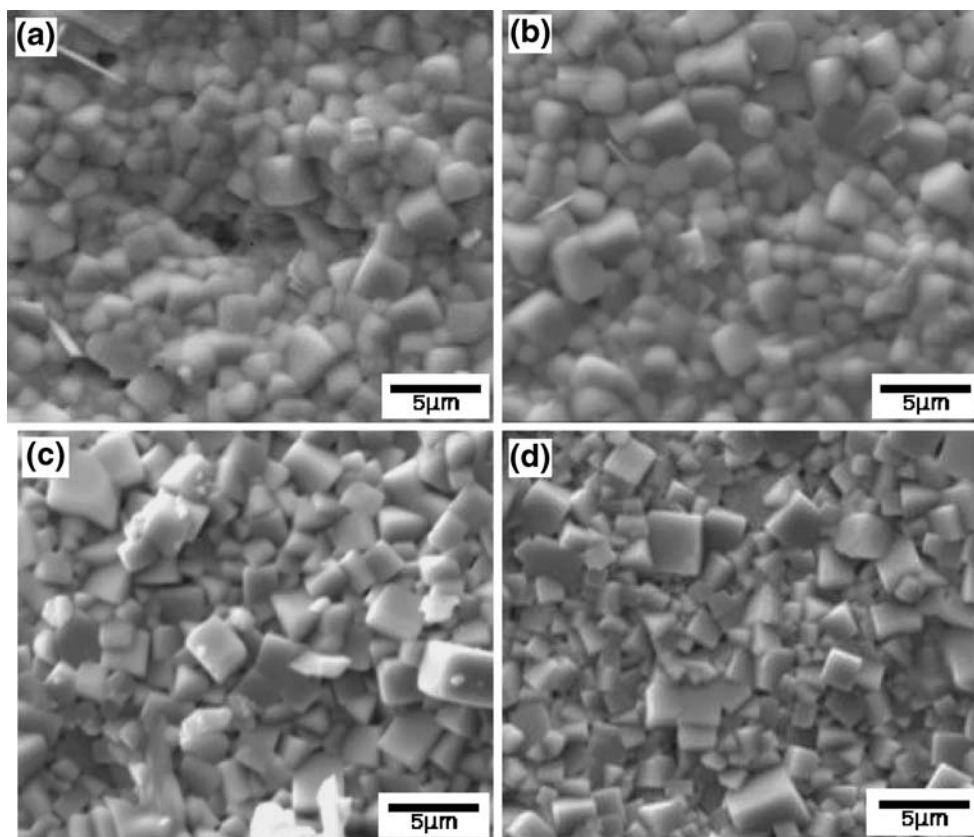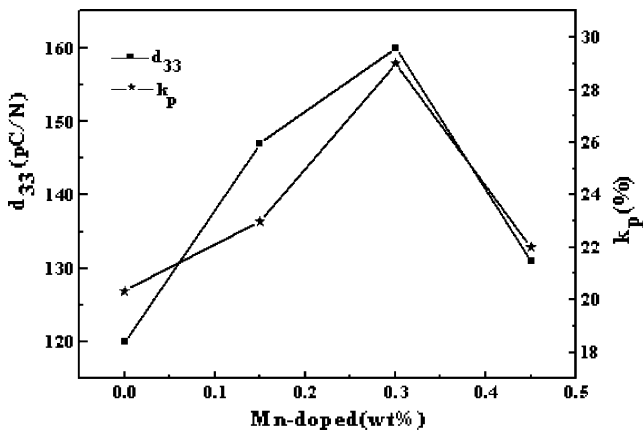
Fig. 4 The piezoelectric constant d_{33} and electromechanical coupling factor k_p of BNBT-6 ceramics sintered at 1160°C as a function of MnO_2 contents

increase of MnO_2 addition. When the amount of MnO_2 is lower than 0.3 wt%, d_{33} and k_p are evidently increased, and the best piezoelectric properties are realized: d_{33}=160 pC/N, k_p=29% for 0.3 wt% MnO_2 content. However, when amount of MnO_2 is more than 0.3 wt%, both d_{33} and k_p show a tendency to decrease with increasing MnO_2 content. It is evident that the electromechanical coupling factor k_p and the piezoelectric constant d_{33} of BNBT-6 +0.3 wt% MnO_2 are further improved compared with un-doped sample (d_{33}=120 pC/N, k_p=20.34%).

Figure 5 shows the variation of the mechanical quality factor Q_m, the dielectric permittivity ε_r and the dissipation factor tan δ of BNBT-6 ceramics sintered at 1160°C dependence of MnO_2 doping. As shown in the Fig. 5, the ε_r increases evidently for $0<x<0.3$ wt%, and then decreases for $x>0.3$ wt%. However, the Q_m shows an opposite change, Q_m decreases evidently for $0<x<0.3$ wt%, and then increases for $x>0.3$ wt%. In the case of tan δ, tan δ increases when x ranges from 0 wt% to 0.15 wt%, and decreases rapidly when x ranges from 0.15 wt% to 0.3 wt%, and then slowly increases when x is over 0.3 wt%. From the Fig. 5, the max value of ε_r is 879, and the min value of tan δ and Q_m are 0.26 and 152 for BNBT-6 doped 0.3 wt% MnO_2, respectively.

When the amount of Mn is lower than 0.3 wt%, considering the valent and ion radius, the manganese ions will go to B-site and create oxygen vacancies as acceptor dopant, which will harden the material. The oxygen vacancies inside the material make the diffusion easier, leading to the good sinterability, increase the density and improve the poling process. Thus the piezoelectric constant d_{33}, the electromechanical coupling factor k_p and the dielectric permittivity ε_r gradually increase by MnO_2 addition. With MnO_2 addition excess, Mn ions are supersaturated in the lattice of BNBT-6, and the excess Mn ions accumulate in the grain boundaries, worsening the

sintering behavior of the ceramics, leading to electrical properties decrease [25].

As a "hard" dopant, Mn doping in BNBT-6 will lead to an increase of Q_m. In the experiment, however, the Q_m shows a tendency to decrease with increasing MnO_2 addition less than 0.3 wt%. The could be owing to the enhancement of domain motion, which causes the increase of inner attrition together with decrease of Q_m. For small MnO_2 addition, the incorporation of smaller cations in a normal perovskite structure causes the slack of lattice and enhances the motion of 90^0 domains [26]. For x>0.3 wt%, the Q_m increases which probably is due to the fact that more Mn ions will substitute for B-site Ti^{4+} ions with the increasing content of Mn. Under this condition, Mn ions are supersaturated in the lattice of BNBT-6, and the excess Mn ions accumulate in the grain boundaries, resulting in a pinning effect on a domain which hinders the motion of a domain [27, 28]. As for the increase of tan δ for x<0.15 wt %, it could be owing to the increase of inner attrition. When x ranges from 0.15 wt% to 0.3 wt%, the transformation of tan δ indicates that MnO_2 is a "hard" doping. For x>0.3 wt%, the sintering behavior of the ceramics is worsen, which cause an increase of tan δ. In addition, according to grain size effect, piezoelectric properties of ceramics are improved with increase of grain size [29]. The grain size gradually increases when x ranges from 0.15 wt% to 0.3 wt % as can be seen in Fig. 3(b) and (c), thus the d_{33} and k_p are enhanced and the tan δ is reduced in the range.

On the base of above experiment results, it can be concluded that MnO_2 doping has remarkably effect on electrical properties of BNBT-6 system and the good piezoelectric properties (d_{33}=160 pC/N, k_p=29%) and the good dielectric properties (ε_r=879, tan δ=2.6%) are obtained for x=0.3 wt%. Compared with the previous paper, the d_{33} and k_p are enhanced in the experiment. The tan δ, however, need further improve in later work.
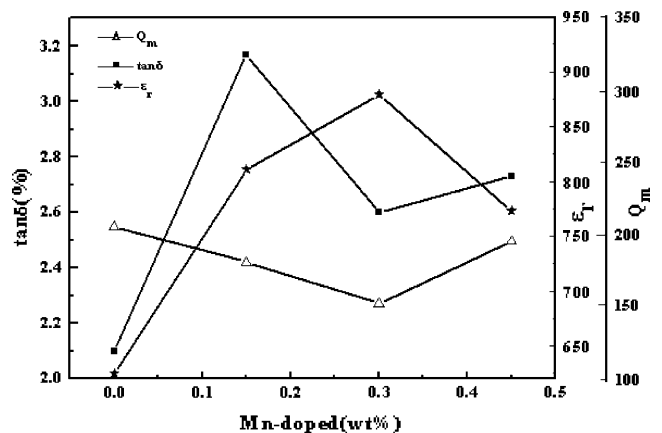

Fig. 5 The mechanical quality factor Q_m, dissipation factor tan δ and dielectric constant of ε_r of BNBT-6 ceramics sintered at 1160°C dependence of MnO_2 contents

4 Conclusion

Microstructure, dielectric and piezoelectric properties of lead-free piezoelectric ceramics BNBT-6 doped with MnO_2 are studied. X-ray diffraction pattern indicates a pure perovskite structure without any secondary impurity phases in BNBT-6+$x$wt%MnO_2 ($x=0\sim0.45$) samples. The dielectric properties and piezoelectric properties are obviously improved. The optimal values are obtained for the BNBT-6 with MnO_2 doping of 0.3 wt%: $\varepsilon_r=879$, $d_{33}=160$ pC/N, $Q_m=152$, $k_p=29\%$ and $\tan\delta=2.6\%$, respectively. These excellent electrical properties of BNBT-6+0.3 wt%MnO_2 ceramics indicate its promising application in electronic devices.

References

1. Y. Saito, H. Takao, T. Tani, T. Nonoyama, K. Takatori, T. Homma, T. Nagaya, M. Nakamura, Nature **432**, 84–87 (2004)
2. T. Takenaka, H. Nagata, J. Eur. Ceram. Soc. **25**, 2693–2700 (2005)
3. G.A. Smolenskii, V.A. Isupov, A.I. Agranovskaya, N.N. Kraink, Sov. Phys. Solid State **2**, 2651–2653 (1961)
4. S.C. Zhao, G.R. Li, A.L. Ding, T.B. Wang, Q.R. Yin, J. Phys. D: Appl. Phys. **39**, 2277–2281 (2006)
5. T. Takenaka, K. Maruyama, K. Sakata, Jpn. J. Appl. Phys. **30**(Part 1 No. 9B) 2236–2239 (1991)
6. D.L. West, D.A. Payne, J. Am. Ceram. Soc. **86**, 192–194 (2003)
7. X.X. Wang, X.G. Tang, H.L.W. Chan, Appl. Phys. Lett. **85**, 91–93 (2004)
8. W. Chen, Y.M. Li, Q. Xu, J. Zhou, J. Electroceram. **15**, 229–235 (2005)
9. Y.M. Li, W. Chen, J. Zhou, Q. Xu, H.J. Sun, R.X. Xu, Mater. Sci. Eng. B **112**, 5–9 (2004)
10. A. Herabut, A. Safari, J. Am. Ceram. Soc. **80**, 2954–2958 (1997)
11. J. Yoo, J. Hong, H. Lee, Y. Jeong, B. Lee, H. Song, J. Kwon, Sensors Actu. A **126**, 41–47 (2006)
12. K. Pengpat, S. Hanphimol, S. Eitssayeam, U. Intatha, G. Rujijanagul, T. Tunkasiri, J Electroceram. **16**, 301–305 (2006)
13. H.D. Li, C.D. Feng, W.L. Yao, Mater. Lett. **58**, 1194–1198 (2004)
14. B.J. Chu, G.R. Li, Q.R. Yin, W.Z. Zhang, D.R. Chen, Acta Phys. Sin. **50**, 2012–2016 (2001)
15. X.X. Wang, H.L.W. Chan, C.L. Choy, Solid State Commun. **125**, 395–399 (2003)
16. S.J. Wu, Q. Xu, X.Z. Zhao, T. Liu, Y.M. Li, Mater. Lett. **60**, 1453–1458 (2006)
17. H. Nagata, M. Yoshida, Y.Makiuchi, T. Takenaka, Jpn. J. Appl. Phys. **42**, 7401–7404 (2003)
18. Y.M. Li, W. Chen, Q. Xu, J. Zhou, X.Y. Gu, Materials Letters **59**, 1361–1364 (2005)
19. S.J. Zhang, T.R. Shrout, H. Nagata, et al. IEEE Trans. Ultrason Ferroelectr. Freq. Control, **54**, 910 (2007)
20. T. Kamiya, T. Suzuki, T. Tsurami, Jpn. J. Appl. Phys. **31**, 3058–3060 (1992)
21. IEEE Standard on Piezoelectricity. (American National Standards Institute, Washington, DC, 1976)
22. H.L. Du, Z.B. Pei, W.C. Zhou, F. Luo, S.B. Qu, Mater. Sci. Eng. A **421**, 286–289 (2006)
23. H. Nagata, T. Takenka, J. Eur. Ceram. Soc. **21**, 1299–1320 (2001)
24. L.S. He, C.E. Li, J. Mater. Sci. **35**, 2477–2480 (2000)
25. S.J. Zhang, R. Xia, T. R. Shrout, Mater. Sci. Eng. **B129**, 131 (2006)
26. P. Roy-Chowdhury, S.B. Deshpande, J. Mater. Sci. **22**, 2209–2211 (1987)
27. W. L. Zhong, Physics of Ferroelectrics. (Science Press, 1996), pp. 274–285
28. T. Kamiya, T. Suzuki, T. Tsurumi, M. Daimon, Jpn. J. Appl. Phys. **31**, 3058–3061 (1992)
29. Y.D. Hou, P.X. Lu, M.K. Zhu, X.M. Song, Mater. Sci. Eng. B **116**, 104–108 (2005)